Supporting Information

A monolayer of primary colonic epithelium generated on a scaffold with a gradient of stiffness for drug transport studies

Dulan B. Gunasekara[1,2], Jennifer Speer[1], Yuli Wang[1], Daniel L. Nguyen[1], Mark I. Reed[1], Nicole M. Smiddy[1], Joel S. Parker[3], John K Fallon[4], Philip C. Smith[4], Christopher E. Sims[1], Scott T. Magness[2], Nancy L. Allbritton[1, 2, *]

[1]Department of Chemistry, University of North Carolina at Chapel Hill, NC 27599, USA

[2]Joint Department of Biomedical Engineering, University of North Carolina at Chapel Hill, NC 27599, USA and North Carolina State University, Raleigh, NC 27607, USA

[3]Department of Genetics and Lineberger Comprehensive Cancer Center, University of North Carolina at Chapel Hill, NC 27514, USA

[4]Division of Pharmacoengineering and Molecular Pharmaceutics, Eshelman School of Pharmacy, University of North Carolina at Chapel Hill, Chapel Hill, North Carolina 27599, USA

*Correspondence to: Nancy L. Allbritton, Email: nlallbri@unc.edu.

Joint Department of Biomedical Engineering, University of North Carolina, Chapel Hill, North Carolina 27599, USA and North Carolina State University, Raleigh, North Carolina 27695, USA.

Tel.: +1-919-966-2291; fax: +1-919-962-2388

Table of Contents

01. Supplemental Methods

02. Supplemental Results

03. Supplemental Figures

Figure S1. A reconstructed confocal stack (z-axis) demonstrating a gradient of fluorescently labeled amine groups along the direction of an Alexa Fluor 594 succinimidyl ester gradient.

Figure S2. Brightfield image of a confluent monolayer

Figure S3. Maturation of the monolayers over time.

Figure S4. Evaluation of whole-genome gene expression in crypts and monolayers.

Figure S5. Conversion of monolayer cultures into organoids provides evidence for the existence of stem/progenitor cells in monolayers.

Figure S6. TEER of monolayers

Figure S7. Heat maps for A) ABC and B) SLC transporters that were significant at FDR of 1%

Figure S8. QTAP SRM quantification and comparison of protein expression of transporters

04. Supplemental Tables

Table 1: A transporter expression comparison of day 5 and crypts vs. day 3 and crypts

05. Supplemental References

Supplemental Methods

Materials. Polystyrene 6-well plates were purchased from Denville Scientific, Inc., Holliston, MA. Collagen (rat-tail), Matrigel, ethylenediaminetetraacetic acid (EDTA), 4-(2-hydroxyethyl)-1- piperazineethanesulfonic acid (HEPES), and gentamicin were purchased from Corning. Dimethyl sulfoxide (DMSO) was acquired from Santa Cruz Biotechnology, Dallas, TX. Optimum cutting temperature (O.C.T.) formulation was obtained from Tissue-Tek, Sakura Finetek USA, Inc., Torrance, CA. 12-well Transwells with polyethylene terephthalate (PET) membranes (pore size 0.4 μm and number of pores $2.0\pm0.2\times10^6/cm^2$), 10× phosphate buffered saline (PBS), Na_2HPO_4, KH_2PO_4, NaCl, KCl, advanced Dulbecco's modified Eagle medium (DMEM)/F-12 medium, dithiothreitol (DTT), GlutaMAX, penicillin, streptomycin, lucifer yellow (LY), rhodamine 123 (Rh123), MultiSpeck™ Multispectral Fluorescence Microscopy Standards Kit and Alexa Fluor™ 594 NHS ester (succinimidyl ester) were from Thermo Fisher Scientific, Waltham, MA. Epidermal growth factor (EGF), N-acetylcysteine, sucrose, D-sorbitol, verapamil, atenolol (ATL), propranolol (PPL), metoprolol (MET) and riboflavin were purchased from Sigma, St. Louis, MO. Collagenase type IV was purchased from Worthington Biochemical Corp., Lakewood, NJ. Information for staining and assay kits is provided in the relevant subsections.

Optimization of gradient cross-liked scaffolds

An EDC-NHS concentration used by others for collagen and shown to work well for primary intestinal stem cell culture (both differentiated and stem cell culture) was used in the basal reservoir[1,2]. In this study, we optimized the reaction time to achieve a gradient of cross-linking spanning the thickness of the scaffold. Mouse epithelial cell attachment to scaffolds was poor when the diffusion/reaction time was greater than 40 min, and scaffolds were deformable by the cells when the diffusion/reaction time was less than 20 min. After the preparation, the gradient cross-linked scaffold could be stored for up to two months (the longest time tested) in 1× PBS and still maintain their ability to support intestinal epithelial cells.

Intestinal stem cell culture medium (SM). SM was prepared by diluting Wnt 3A, R-spondin 2 and Noggin-conditioned medium in advanced DMEM/F-12 medium and adding necessary nutrients and buffers. The conditioned medium was prepared as described previously.[1] The final concentrations of SM additives were Wnt 3A (80 ng/mL), R-spondin 2 (38 ng/mL), Noggin (36 ng/mL), GlutaMAX (1×), HEPES (10 mM), N-acetyl cysteine (1.25 mM), murine EGF (50 ng/mL), penicillin (100 unit/mL), streptomycin (100 μg/mL), gentamicin (50 μg/mL) and A83-01 (500 nM). The concentrations of Wnt 3A, R-spondin 2 and Noggin were

measured as described previously.[1] The cell expansion medium (EM) was identical to SM but without A83-01.

Isolation of crypts from mouse colons. The cytomegalovirus enhancer plus chicken actin promoter (CAG)-DsRed mouse model in which all cells express the fluorescent protein DsRed, and wild-type (WT) mice were used for experiments.[1,3] All experiments and animal usage were in compliance with the University of North Carolina Animal Care and Use Committee (IACUC) and all animal protocols were approved by the IACUC. CAG-DsRed mice were bred on a CD-1 background and WT mice were bred on a C57BL/6 background. Mice (both male and female, age 6-10 weeks) were humanely euthanized by a lethal dose of isoflurane followed by cervical dislocation under the UNC IACUC-approved protocol #13-200. A detailed procedure for isolation of crypts was previously reported by our group.[4] Briefly, surgically extracted colon was opened longitudinally and incubated with EDTA (2 mM) and DTT (0.5 mM) in isolation buffer (5.6 mM Na_2HPO_4, 8.0 mM KH_2PO_4, 96.2 mM NaCl, 1.6 mM KCl, 43.4 mM sucrose, 54.9 mM D-sorbitol, pH 7.4) for 75 min at room temperature. The tissue was vigorously shaken to loosen crypts from underlying stroma. Released crypts were then isolated by centrifugation.

Monolayer culture of colonic epithelial cells. Colonic crypts were mixed with SM (3 mL) and plated on the neutralized collagen hydrogel at a density of 1,000 crypts/cm^2 per well. At day 2, SM was replenished (4 mL). At day 3, the cells were sub-cultured into new wells by digesting the collagen scaffold with collagenase (type IV, 500 U/mL, Worthington Biochemical, LS004189). After digestion, the monolayers were washed by centrifugation (0.8 × g for 1 min) and disassociated into small groups of cells by incubation with EDTA (0.5 mM) and Y-27632 (10 μM, Rho-associated protein kinase inhibitor, Sigma) in PBS. The cells were then split 1:2 into wells of a 6-well plate (900,000 cells/cm^2). Cells that attached to the collagen surface spread by 2 days. The SM was replenished at day 2. At day 3-4 cells were again sub-cultured as above.

Interconverting cell monolayers and organoids. To demonstrate the presence of proliferative cells, confluent monolayers (day 5, TEER 1410 ± 1009 Ω cm^2, n=3 monolayers) were isolated, broken into smaller pieces and embedded in Matrigel. Organoids formed in the initial passage (P0) and were isolated at day 5 and sub-cultured every 5 days for 3 passages.

Fluorescent staining of cells. Confluent monolayers derived from the tissue of a WT mouse were stained at days 2 through 5 to assess the presence of S-

phase cells, mucin-2 (Muc2), alkaline phosphatase (ALP) and DNA as described previously.[1] Sections (10 μm-thick) of the monolayers obtained using a cryostat (OFT5000, Bright Instruments, UK) were stained for actin, E-cadherin, and integrin β4 as described previously.[1]

Three separate monolayers were used on each day. Briefly, monolayers were pulsed with EdU for 6 h after the TEER measurement was made. The living monolayers were then incubated with ALP substrate (Vector Laboratories, Burlingame, CA) in Tris buffer (0.15 M, pH 8.4) for 30 mins. The monolayers were fixed with paraformaldehyde (4%) for 25 min then incubated with Click-iT EdU Alexa Fluor 647 reagent (Thermo Fisher Scientific, Waltham, MA) to label cells incorporating EdU. The cells were then immunostained with rabbit anti-mucin2 antibody (α-Muc2, 1:200, Santa Cruz Biotechnology, Inc, Dallas, Texas, #sc-15334) followed by a secondary antibody, Alexa Fluor 488 α-rabbit (1:500, Jackson Immunoresearch, West Grove, PA, # 711-545-152). DNA was then stained by incubation with Hoechst 33342 (1 μg/mL). Samples were stored in PBS with 0.5% azide at 4°C until imaged.

Prior to sectioning, fixed cells were treated with 30% sucrose for 3 h followed by O.C.T. formulation overnight. Monolayer sections were stained with fluorescently-labeled phalloidin for F-actin (ActinGreen™ 488, Molecular Probes, Thermo Fisher Scientific, Waltham, MA) and rabbit polyclonal anti-integrin β4 antibody (1:200) with a secondary antibody, donkey anti-rabbit IgG conjugated with Alexa Fluor 594 (1:500, Jackson Immunoresearch). E-cadherin was immunolabeled using rabbit polyclonal anti-E-cadherin and ZO-1 antibody (2.5: 200 and 1:200 dilution, respectively, Protein Tech) followed by staining with a secondary antibody, donkey anti-rabbit IgG conjugated with Alexa Fluor 594 (2:500).

Fluorescence and brightfield imaging. Prior to imaging, a software-based autofocus scan was performed using Hoechst 33342 fluorescence to determine the optimum focal positions throughout the sample.[5] The fluorescence of the Hoechst 33342, ALP reagent, EdU label, and Muc2 immunostain was obtained using blue, red, far red, and green filter sets, respectively (Chroma ET-DAPI 49000, Semrock TxRed-4040B, Chroma ET-Cy5 49006, and Semrock FITC-3540B). High resolution fluorescence and brightfield images were obtained using a Nikon Eclipse TE300 inverted epifluorescence microscope with an estimated objective depth-of-field of 11 μm (10× N.A. 0.3) and an Olympus Fluoview FV3000 confocal laser scanning microscope using 20× (N.A. 0.45) or 40× (N.A. 0.95) UPLSAPO objectives.

Fluorescence image analysis. Well-focused center portions of images from a monolayer were stitched together for automated image analysis.[5] Custom MATLAB scripts were used for both stitching and area analysis. To determine cell coverage, the stained area of stitched fluorescence images was filtered using a low pass filter (wiener2, MATLAB) to remove the noise and then the background was subtracted (Top-hat, MATLAB). Next, images were manually thresholded to obtain the stained area. The stained area divided by the Hoechst 33342 area was used to estimate the percentage of area covered by cells displaying each stain.

Assessment of the feasibility of forming a gradient of reactants across a collagen scaffold. Since the diffusion of EDC/NHS through the collagen could not be visualized, Alexa Fluor 594 succinimidyl ester, which possesses a similar molecular weight, was used to assess the feasibility of forming a gradient of reaction products through the collagen scaffold. As described above, a collagen scaffold was formed in a Transwell, and the plate was placed at 4°C for 30 min. Alexa Fluor 594 succinimidyl ester (5 µg/mL in PBS) was added to the lower compartment and the upper compartment was filled with PBS. The scaffold was maintained at 4°*C* for 40 min to permit the Alexa Fluor 594 succinimidyl ester to diffuse into and react with amine groups in the collagen scaffold. After 40 min, the scaffold was washed with PBS and imaged using a confocal microscope (Olympus FluoView FV3000, 20×, N.A. 0.45). Prior to imaging, multicolor fluorescence beads (4 µm) were placed on the scaffold to mark the top surface.

Measurement of scaffold stiffness. Scaffold stiffness was measured in the presence of PBS using atomic force microscopy (AFM, Asylum Research MFP3D). A force (100-500 pN) was applied perpendicular to the scaffold surface using a 2.25 µm polystyrene spherical bead mounted on a 30 pN/nm silicon nitride cantilever (Novascan Technologies, Inc.), and the cantilever's displacement in response to the applied force was measured. The spring constant of the cantilever was determined prior to each experiment using a thermal tune method (total average spring constant of 3 cantilevers: 28.76 ± 1.29 pN/nm). For each scaffold tested, force *vs.* displacement curves were recorded at ≥10 different positions across the surface with 5 measurements taken at each position. Five different scaffolds were used for each experimental group. To determine stiffness, force *vs*. indentation curves were fit using the Hertz model.[6] Scaffolds used for stiffness measurements included collagen cross-linked in a gradient, non cross-linked collagen and Matrigel. Scaffolds made in Transwells (all except Matrigel) were cut and removed with the permeable membrane. Before beginning AFM measurements, all scaffold samples were deposited on

microscope glass slides and secured in place using an O-ring made from polydimethylsiloxane (PDMS, Dow Corning).

Supplemental Results

Characterization of monolayers by mRNA expression. Whole transcriptome expression analysis was used to compare native crypt tissue to the monolayers as they grew to cover the scaffold. Evaluation of the RNA sequence data between samples by principal component analysis suggested that the gene expression of the day-5 monolayers was most similar to that of the *in vivo* epithelium relative to that of monolayers cultured for shorter times (SI Figure 3). To understand why the mature monolayers most resembled *in vivo* tissue, mRNA expression of genes characteristic of intestinal stem/proliferative and differentiated cells was assayed and compared to that of freshly obtained colonic epithelium (Figure 2F). Stem/proliferative cells such as that found at the crypt base in the proliferative cell zone of *in vivo* crypts express significant levels of Lgr5, Hopx, Bmi1, Lrig1, Tert, prom 1, Ephb2, and Sox 9. These genes were observed in all of the monolayer cultures although to the greatest degree in the early stage, highly-proliferative, monolayers that did not yet fully cover the scaffold (Figure 2A). Although Lgr5 gene expression significantly decreased over the monolayer culture time, isolated cells from day 5 monolayers could be grown as organoids and subcultured for multiple passes suggesting that some stem cells might have remained the in day 5 cultures (Figure S5). Gene expression of the various differentiated cells (mucous-secreting goblet cells, hormone-secreting enteroendocrine cells, and absorptive enterocytes) was also assessed. Monolayers at all days in culture demonstrated mRNA expression consistent with the presence of these expected cell lineages, but the greatest expression occurred in the day-5 cultures that had fully covered the scaffold. These data suggested that the cells of the monolayer became increasingly differentiated as they reached confluency in a manner similar to native epithelium which is comprised primarily of mature differentiated cells.

Paracellular and transcellular transport of the substrates ATL and PPL. Paracellular and transcellular transport of the substrates ATL and PPL were used for comparison of our mouse monolayers to that found in mouse *in vivo* colonic tissue. PPL transport was similar to that of *in vivo* mouse colon (table below).[7–10] ATL transport by the mouse monolayers was lower than that of *in vivo* mouse colon but similar to that for Caco-2 cells are ~1×10^{-7} cm s^{-1}.[7–9]

Drug	Mouse Monolayers (cm s^{-1})	*In Vivo* Mouse Colon (cm s^{-1})	Caco 2 cell data (cm s^{-1})	References
PPL	1×10^{-5}	$5.6\text{-}7.0 \times10^{-5}$	$0.4\text{-}2.5 \times10^{-5}$	7-10
ATL	$<1.2 \times10^{-7}$	$100\text{-}180 \times10^{-7}$	$2\text{-}10 \times10^{-7}$	7-9

Figure S1.

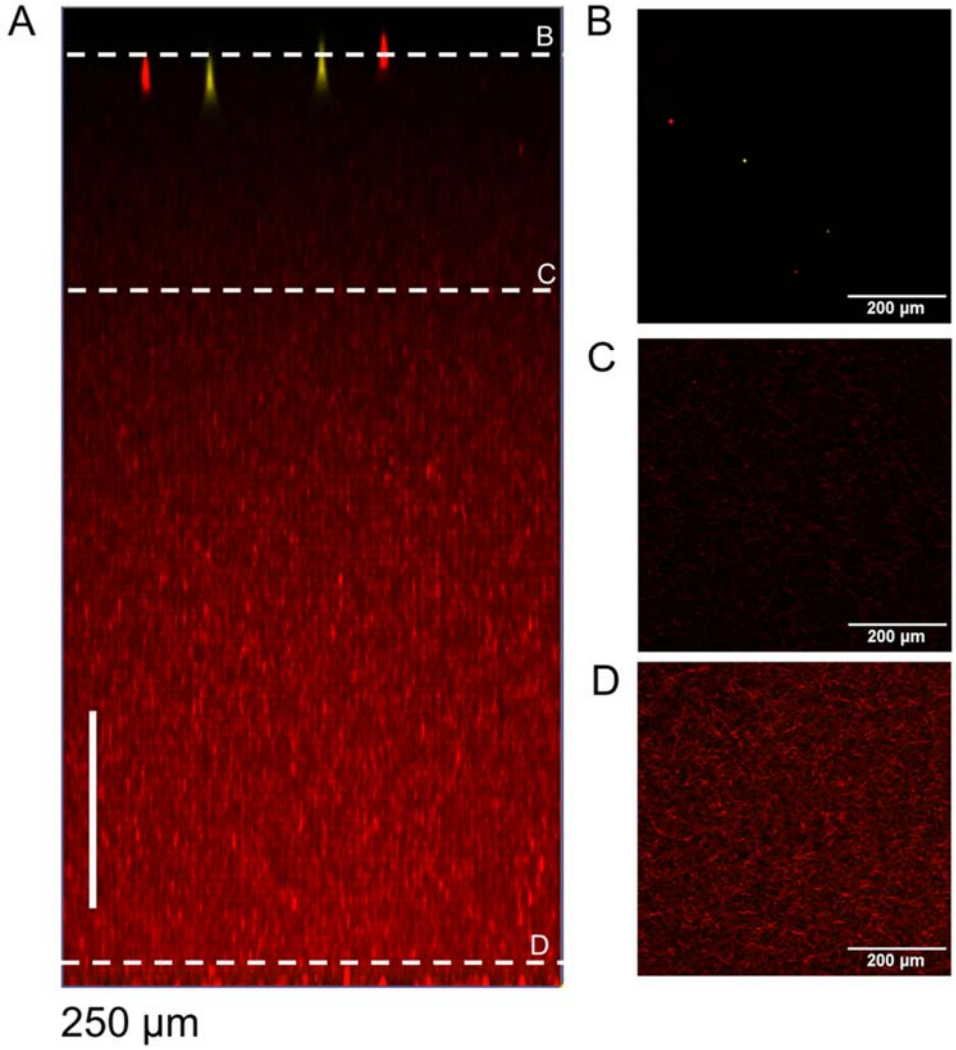

Figure S1. A) A reconstructed confocal stack (z-axis) that shows a gradient of fluorescently labeled amine groups along the direction of an Alexa Fluor 594 succinimidyl ester gradient. 1.5 mL of 5 µg/mL Alexa Fluor 594 succinimidyl ester in 1× PBS was added into lower reservoir of a Transwell cassette and the upper reservoir contained 0.5 mL 1× PBS (above the collagen scaffold on the porous membrane of the Transwell insert). The cassette was stored at 4 °C for 40 min to allow the amine-reactive fluorophore to diffuse through the membrane and scaffold. The ester reacts with free amine groups in collagen while it diffuses through the scaffold. Multicolor fluorescence beads (4 µm) were placed on the scaffold to mark the top surface. B-D) X-Y slices through the scaffold at the locations indicated in panel A.

Figure S2.

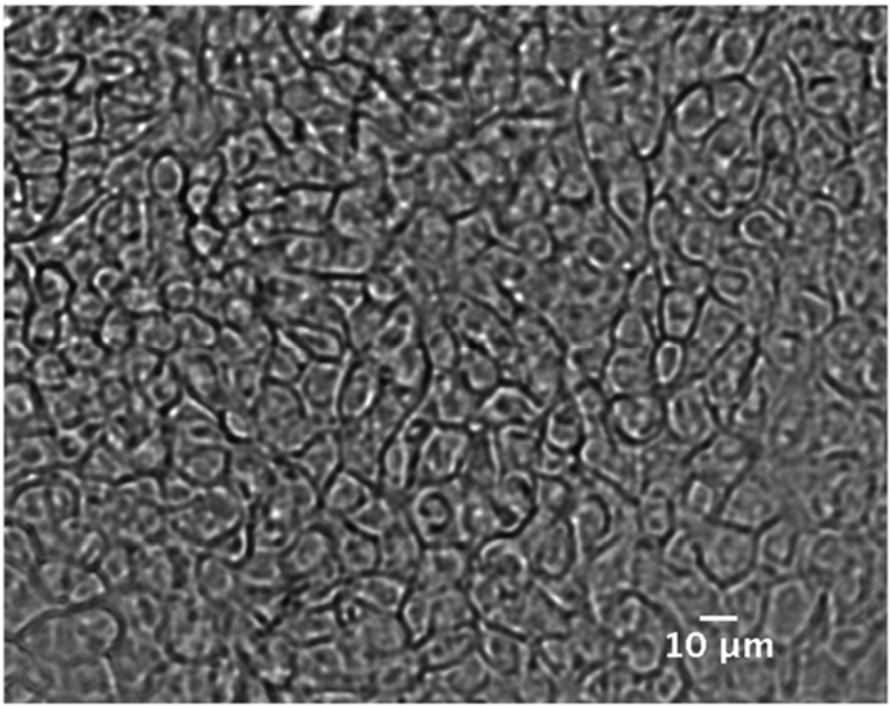

Figure S2. Brightfield image of a region of a confluent monolayer shows tightly packed cells.

Figure S3.

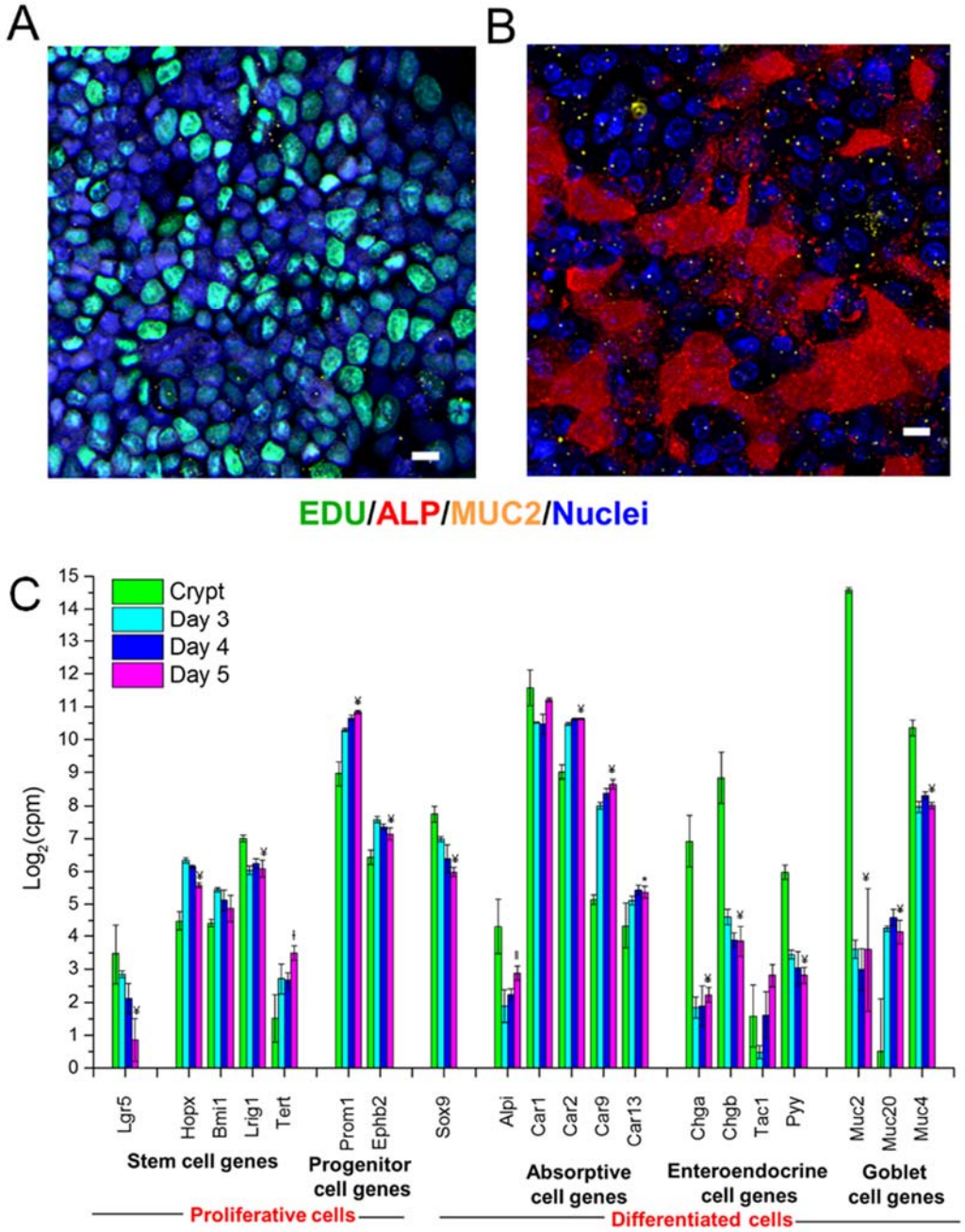

Figure S3. Maturation of the monolayers over time. A & B) Confocal images of stained monolayers for proliferative cells (green, EdU), enterocytes (red, ALP), goblet cells (yellow/orange, Muc2) and nuclei (blue, Hoechst 33342) at day 2 with TEER 20.7 (A) and day 5 with TEER 1197 Ω cm^2 (B). The scale bar is 20 μm. C) A comparison of mRNA expression levels for stem/proliferative cells, enterocytes, enteroendocrine cells and goblet cell markers in colonic monolayer over time. Statistical significance (P_{adj}) between crypts and day 5 monolayers is labeled with symbols as defined in methods.

Figure S4.

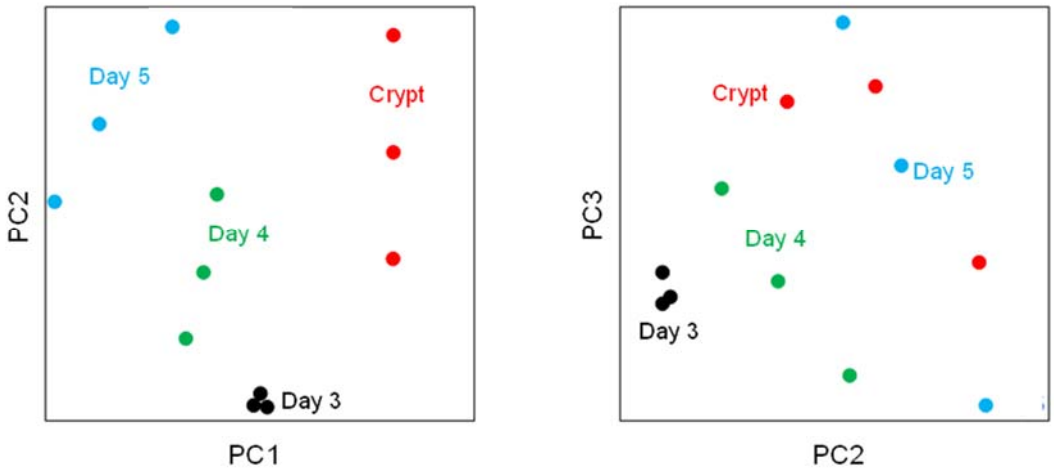

Figure S4. Evaluation of whole-genome gene expression in crypts and monolayers at different culture times using principle component analysis. A) PC1 and 2 segregates the crypt samples from all the others, while B) PC2 and PC3 show higher correlation between the crypt (red) and day 5 (blue) samples compared to day 3 (black) and 4 (green).

Figure S5.

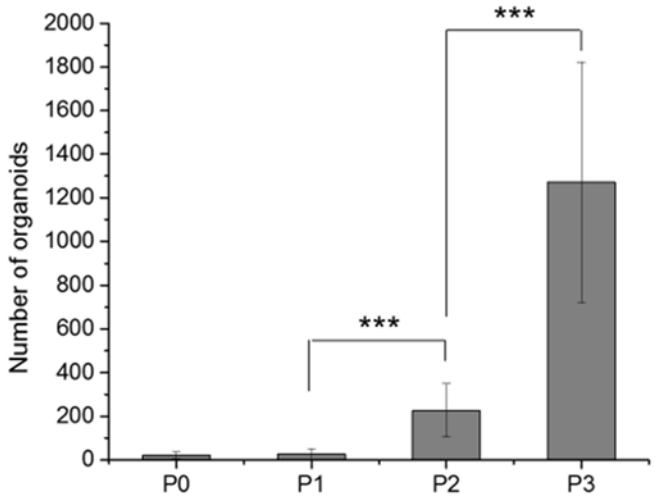

Figure S5. Conversion of 5-day monolayer cultures into organoids provides evidence of the existence of stem/progenitor cells in monolayers at day 5. The histograms show the number of organoids generated using cells isolated from monolayers at day 5. P0 marks the first subculture of the monolayer cells in a Matrigel patty and P1 to P3 are respective subcultures.

Figure S6.

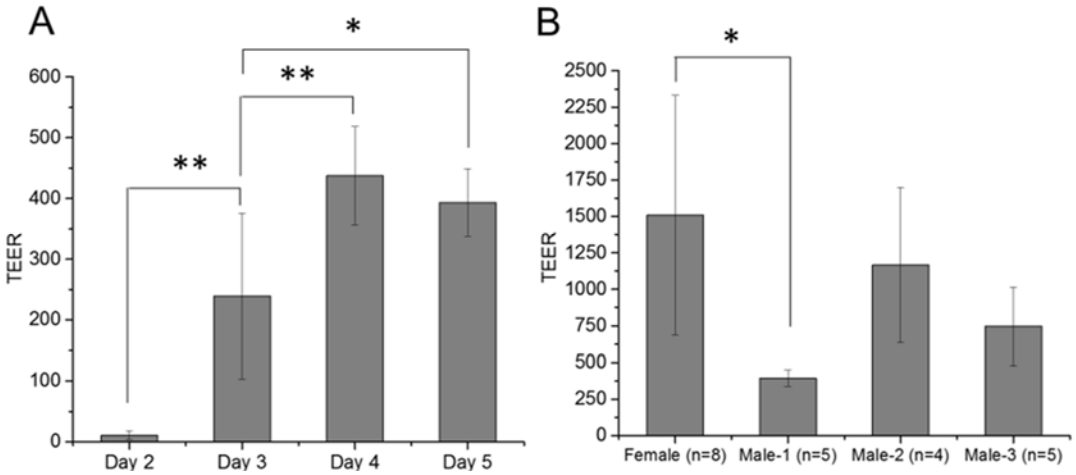

Figure S6. TEER of monolayers. A) A comparison of monolayer TEER overtime and B) mouse-to-mouse TEER variability. Comparison of TEER data from the mice shows only the female and original male mouse were statistically different ($p=0.0144$) in panel B.

Figure S7.

Panel A

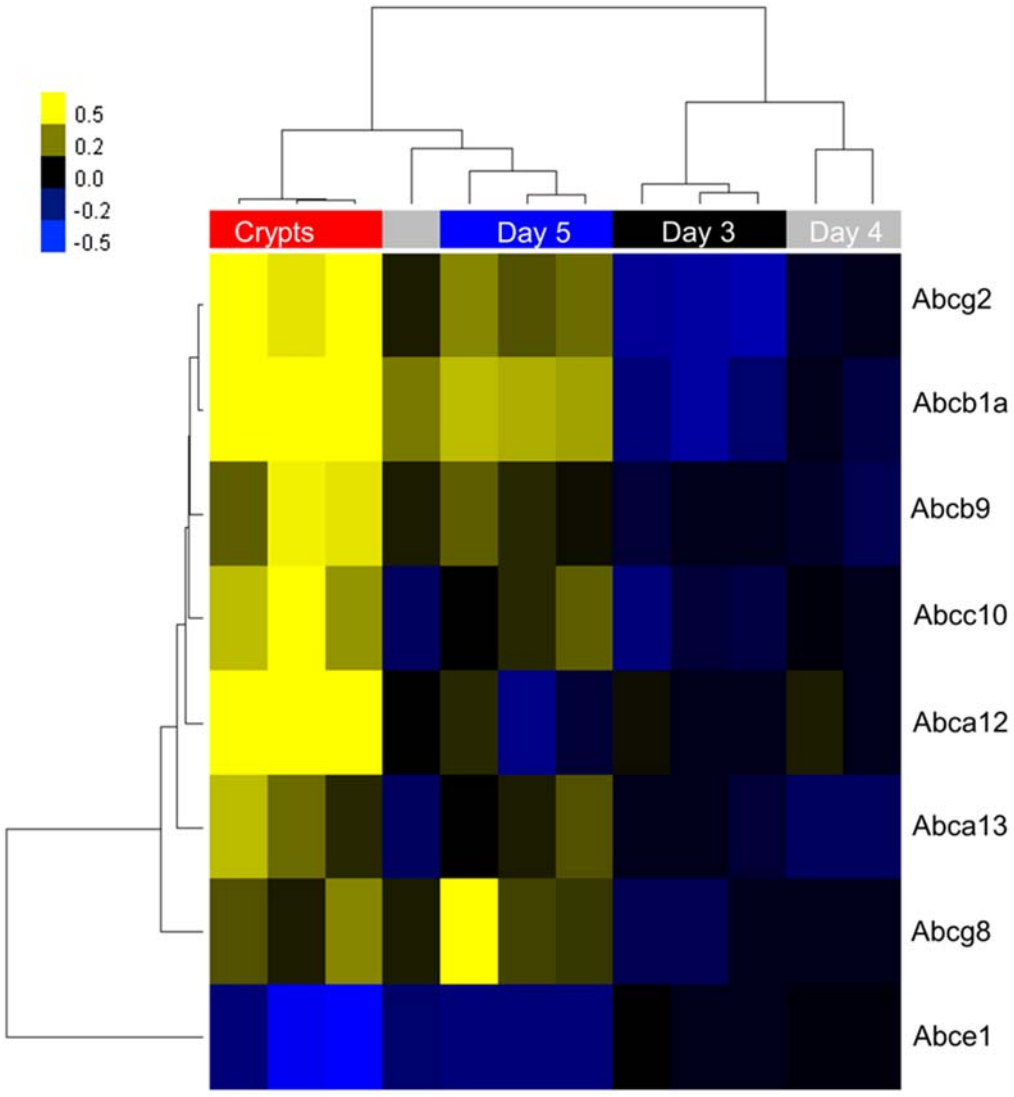

Panel B

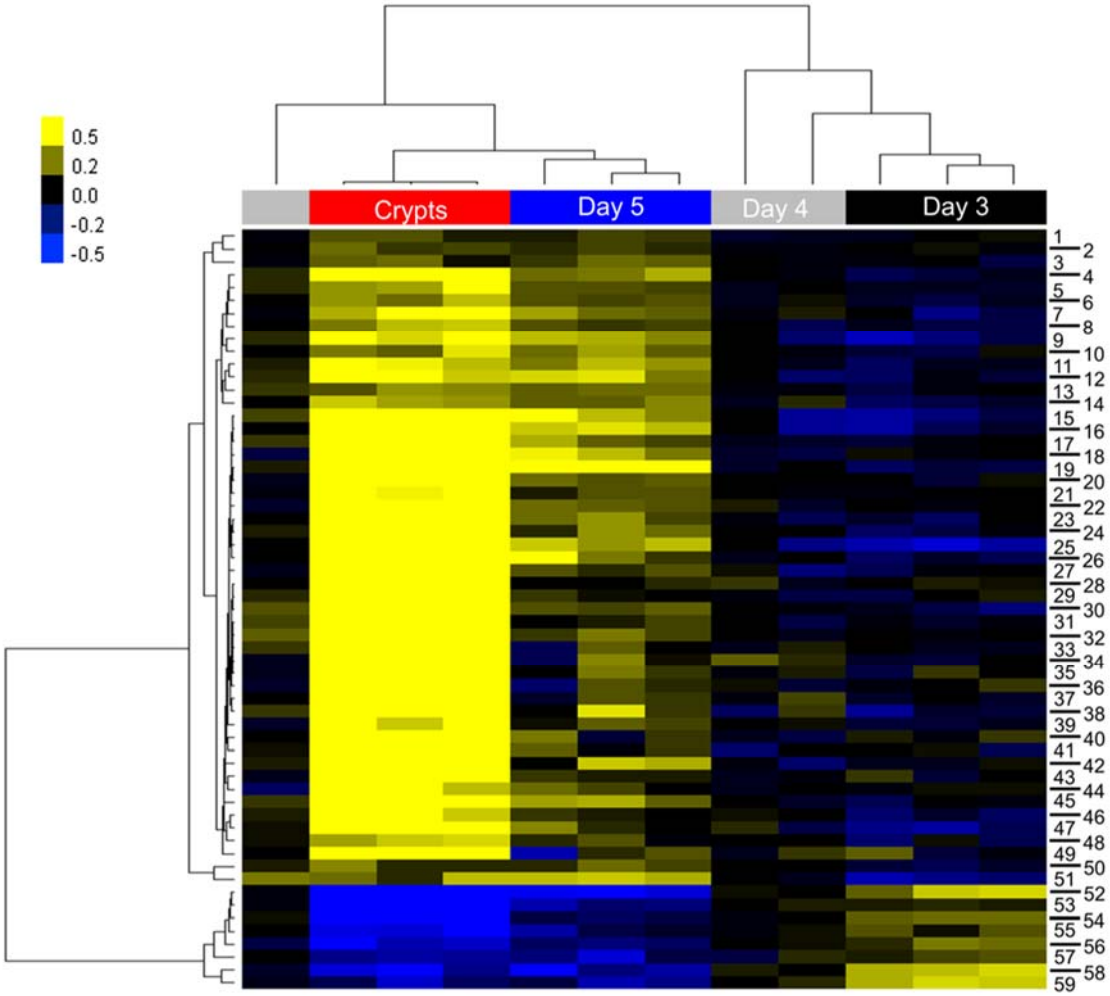

Figure S7. Heat maps for A) ABC and B) SLC transporters that were significantly changed across the time points at an FDR of 1%. The upper horizontal color bands above each heat map designate the column samples: Crypt: **red**, Day 3:**black**, Day 4:**gray**, Day 5:**blue.**

1: Slc 35e1, 2: Slc25a22, 3: Slc7a8, 4: Sla20a1, 5: Slc16a1, 6: Slc9a8, 7: Slc9a1, 8: Slc44a4, 9: Slc30a1, 10: Slc6a8, 11: Slc12a6, 12: Slc9a2, 13: Slc35d1, 14: Slc37a1, 15: Slc25a20, 16: Slc5a1, 17: Slc39a5, 18: Slc51b, 19: Slc13a2, 20: Slc51a, 21: Slc5a8, 22: Slc39a8, 23: Slc25a35, 24: Slc8a1, 25: Slc1a1, 26: Slc41a2, 27: Slc15a1, 28: Slc39a9, 29: Slc25a10, 30: Slc25a34, 31: Slc6a14, 32: Slc16a5, 33: Slc9a3, 34: Slc10a5, 35: Slc4a2, 36: Slc26a3, 37: Slc26a2, 38: Slc12a7, 39: Slc37a2, 40: Slco2a1, 41: Slc13a1, 42: Slc7a9, 43: Slc2a13, 44: Slc36a1, 45: Slc25a23, 46: Slc27a4, 47: Slc30a10, 48: Slc25a42, 49: Slc22a18, 50: Slc3a1, 51: Slc2a4rg-ps, 52: Slc7a5, 53: Slc7a1, 54: Slc6a9, 55: Slc1a4, 56: Slc7a11, 57: Slc3a2, 58: Slc25a4, 59: Slc44a2

Figure S8.

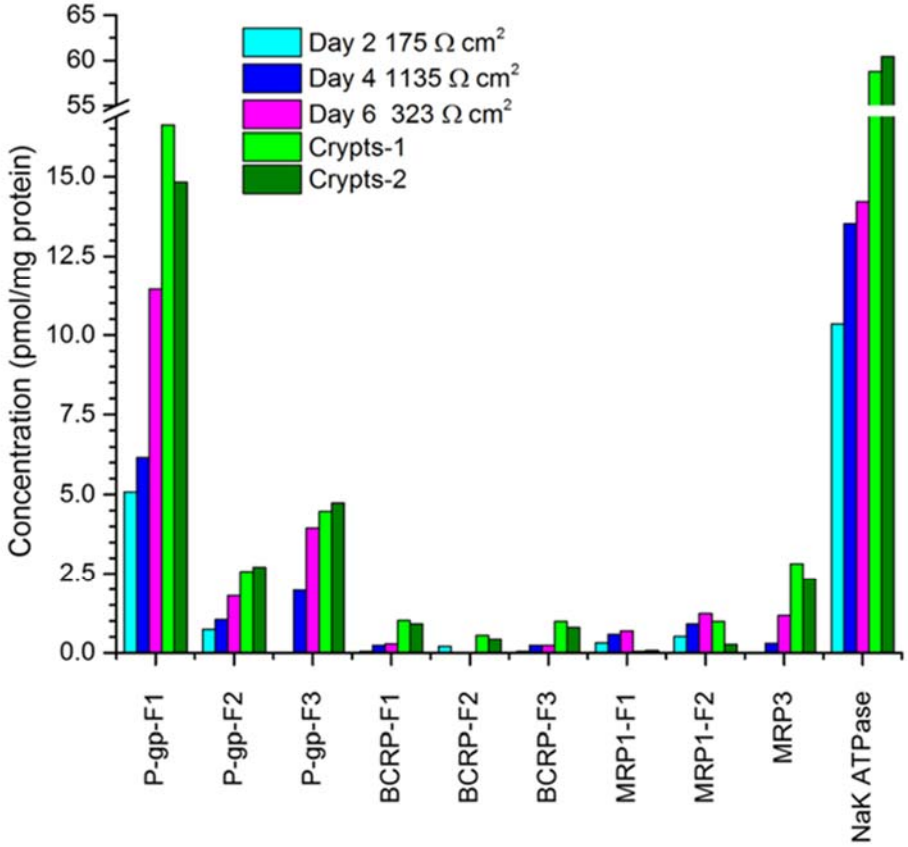

Figure S8. QTAP SRM quantification and comparison of protein expression of transporters in the crypts and confluent monolayers at different days in culture. Concentrations of peptide fragments related to transporters are shown.

Supplemental Table

Table 1. Peptide markers of transporter proteins and QTAP SRM parameters used for quantification of transporters in monolayers and crypts.[11,12]

Abbrev-iation	Peptide	Residual position	Precursor ion 1	Precursor ion 2	Product ion	
					1	2
P-gp-F1	NTTGALTTR	809–817	472.76	-	729.41 (y7)	628.36 (y6)
P-gp-F2	IATEAIENFR	896−905	587.31	-	759.40 (y6)	688.37 (y5)
P-gp-F3	QLNVQWLR	809-816	533.81	-	612.35 (y4)	825.46 (y6)
BCRP-F1	SSLLDVLAAR	87-96	527.81	-	654.38 (y6)	767.47 (y7)
BCRP-F2	ENLQFSAALR	138-147	579.81	-	674.39 (y6)	802.45 (y7)
BCRP-F3	LFDSLTLLASGK	251-262	636.87	-	1012.58 (y10)	697.43 (y7)
MRP1-F1	TPSGNLVNR	1067-1075	484.26	-	433.74 (y8)	769.42 (y7)
MRP1-F2	AYYPSIVANR	1188-1197	582.31	-	766.45 (y7)	398.17 (b3)
MRP3-F1	GALVAVVGPVGCGK	654-667	646.37	-	682.35 (y7)	781.42 (y8)
NaK ATPase-F1	VDNSSLTGESEPQTR	213-227	543.92	815.38	511.29 (y4)	511.29 (y4)

Supplemental References

(1) Wang, Y.; DiSalvo, M.; Gunasekara, D. B.; Dutton, J.; Proctor, A.; Lebhar, M. S.; Williamson, I. A.; Speer, J.; Howard, R. L.; Smiddy, N. M.; et al. Self-Renewing Monolayer of Primary Colonic or Rectal Epithelial Cells. *Cell. Mol. Gastroenterol. Hepatol.* **2017**, *4*, 165–182.

(2) Wang, Y.; Gunasekara, D. B.; Reed, M. I.; DiSalvo, M.; Bultman, S. J.; Sims, C. E.; Magness, S. T.; Allbritton, N. L. A Microengineered Collagen Scaffold for Generating a Polarized Crypt-Villus Architecture of Human Small Intestinal Epithelium. *Biomaterials* **2017**, *128*, 44–55.

(3) Gracz, A. D.; Ramalingam, S.; Magness, S. T. Sox9 Expression Marks a Subset of CD24-Expressing Small Intestine Epithelial Stem Cells That Form Organoids in Vitro. *AJP Gastrointest. Liver Physiol.* **2010**, *298*, G590–G600.

(4) Ahmad, A. A.; Wang, Y.; Gracz, A. D.; Sims, C. E.; Magness, S. T.; Allbritton, N. L. Optimization of 3-D Organotypic Primary Colonic Cultures for Organ-on-Chip Applications. *J. Biol. Eng.* **2014**, *8*, 1–10.

(5) Gunasekara, D. B.; DiSalvo, M.; Wang, Y.; Nguyen, D. L.; Reed, M. I.; Speer, J.; Sims, C. E.; Magness, S. T.; Allbritton, N. L. Development of Arrayed Colonic Organoids for Screening of Secretagogues Associated with Enterotoxins. *Anal. Chem.* **2018**, *90*, 1941–1950.

(6) Sokolov, I. Atomic Force Microscopy in Cancer Cell Research. *Cancer Nanotechnol.* **2007**, *1*, 1–17.

(7) Da Silva, L. C.; Da Silva, T. L.; Antunes, A. H.; Rezende, K. R. A Sensitive Medium-Throughput Method to Predict Intestinal Absorption in Humans Using Rat Intestinal Tissue Segments. *J. Pharm. Sci.* **2015**, *104*, 2807–2812.

(8) Yamaura, Y.; Chapron, B. D.; Wang, Z.; Himmelfarb, J.; Thummel, K. E. Functional Comparison of Human Colonic Carcinoma Cell Lines and Primary Small Intestinal Epithelial Cells for Investigations of Intestinal Drug Permeability and First-Pass Metabolism. *Drug Metab. Dispos.* **2016**, *44*, 329–335.

(9) Wang, X.-X.; Liu, G.-Y.; Yang, Y.-F.; Wu, X.-W.; Xu, W.; Yang, X.-W. Intestinal Absorption of Triterpenoids and Flavonoids from Glycyrrhizae Radix et Rhizoma in the Human Caco-2 Monolayer Cell Model. *Molecules* **2017**, *22*, 1627.

(10) Nagare, N.; Damre, A.; Singh, K.; Mallurwar, S.; Iyer, S.; Naik, A.; Chintamaneni, M. Determination of Site of Absorption of Propranolol in Rat Gut

Using in Situ Single-Pass Intestinal Perfusion. *Indian J. Pharm. Sci.* **2010**, *72*, 625.

(11) Fallon, J. K.; Neubert, H.; Hyland, R.; Goosen, T. C.; Smith, P. C. Targeted Quantitative Proteomics for the Analysis of 14 UGT1As and-2Bs in Human Liver Using NanoUPLC–MS/MS with Selected Reaction Monitoring. *J. Proteome Res.* **2013**, *12*, 4402–4413.

(12) Prasad, B.; Unadkat, J. D. Optimized Approaches for Quantification of Drug Transporters in Tissues and Cells by MRM Proteomics. *AAPS J.* **2014**, *16*, 634–648.